A Method for Identifying Human-generated Forces during an Extensor Thrust

Seong-Wook Hong[1,#], Vlad Patrangenaru[2], William Singhose[2] and Stephen Sprigle[3]

1 School of Mechanical Engineering, Kumoh National Institute of Technology, Kumi, Kyungbuk, South Korea
2 School of Mechanical Engineering, Georgia Institute of Technology, Atlanta, Georgia, USA
3 Center for Assistive Technology and Environmental Access (CATEA), Georgia Institute of Technology, Atlanta, Georgia, USA
Corresponding Author / E-mail: swhong@kumoh.ac.kr, Tel: +82-54-478-7344, Fax: +82-54-478-7139

KEYWORDS : Extensor thrust, Wheelchair, Dynamic seat, Inverse dynamic approach, Human-generated forces

Some wheelchair users with neuromuscular disorders experience involuntary extensor thrusts, which may cause injuries via impact with the wheelchair, cause the user to slide out of the wheelchair seat, and damage the wheelchair. Knowledge of the human-generated forces during an extensor thrust is of great importance in devising safer, more comfortable wheelchairs. This paper presents an efficient method for identifying human-generated forces during an extensor thrust. We used an inverse dynamic approach with a three-link human body model and a system for measuring human body motion. We developed an experimental system that determines the angular motion of each human body segment and the force at the footrest, which was used to overcome the mathematical indeterminacy of the problem. The proposed method was validated experimentally, illustrating the force-identification process during an extensor thrust.

Manuscript received: December 9, 2005/ Accepted: April 20, 2006

1. Introduction

People with neuromuscular disorders can undergo involuntary extensor thrusts, which involve the simultaneous contraction of nearly all of their muscles. Consequently, the body tends to straighten, as shown in Fig. 1, and a user can slide out of the wheelchair seat during an extensor thrust. The commonly used treatment is to restrain the users in their wheelchairs, although this is painful. While research on wheelchairs has examined long-term use, the prevention of secondary injuries, and greater personal freedom,[1] few studies have specifically examined wheelchairs for people subject to severe extensor thrust. Recently, the concept of a "dynamic seating system," which allows movement with respect to the wheelchair frame during an extensor thrust, has been proposed as a potential solution[2] and products based on the dynamic seat concept are available.[3,4] However, most of these products appear to be designed empirically only to prevent wheelchair breakage.

Some attempts have been made to measure the forces resulting from an extensor thrust, including those to measure the spasticity at the elbow,[5] develop a passive dynamic model of the knee joint affected by spastic paresis,[6] and determine a quantitative measure of muscle spasticity using the pendulum knee drop test.[7] However, little is known about the motion and forces during an unconstrained total-body extensor thrust. One reason is because it is very difficult to measure the human-generated forces directly. This paper proposes an inverse dynamic approach to identify the human-generated forces indirectly using limited measurements of forces and the motion of wheelchair users during extensor thrust events.

The inverse dynamic approach has played an important role in estimating the forces acting on the human body. Using this approach, many researchers have been able to obtain joint forces and moments in biomechanical studies of locomotion, *e.g.*, sit-to-stand, jumping, gait, and running.[8,9] In this study, the dynamics of the human body during extensor thrust events were subject to a special set of kinematic constraints because the chair constrains the motion. The lack of information about the reaction forces with the chair makes the problem mathematically indeterminate, a problem affecting many biomechanical studies.[10,11] We used force measurements at the footrest to make the problem mathematically determinate.

We proposed a method for identifying the human-generated forces during extensor thrust events. An experimental system was developed to measure the motion of the human body and the normal force at the footrest. The proposed method is capable of identifying the human-generated forces using inverse dynamic analysis with the

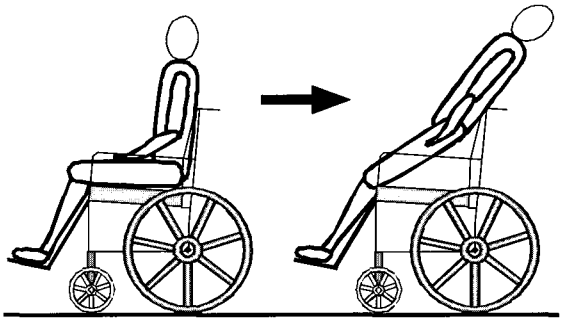

Fig. 1 Body straightening during an extensor thrust

help of the measured foot force and motion. The proposed method was demonstrated using simulations and experimental results obtained from people pretending to undergo extensor thrusts.

A preliminary experiment was performed to validate the proposed dynamic model. Additional experiments demonstrated the identification of human-generated forces during extensor thrust events.

2. Dynamic Modeling and Identification Method

2.1 Equations of Motion

Assumptions are introduced to derive a simple yet meaningful dynamic model, based on careful observations and the analysis of extensor thrusts. First, the dynamic model is confined to extension motion in the sagittal plane, which appears to be the most common and dominant. Second, the human body is assumed to have, without loss of generality, three rigid segments (the lower leg, thigh, and torso) and the associated joints (the ankle, knee, and hip). Third, the chair is assumed to be rigid. Fourth, the ankle is assumed to be a hinged, torque-free pivot point. This assumption is not strictly true for some people with severe calf muscle extension. However, it does not greatly affect the results as long as the ankle torque is sufficiently less than the knee and hip torques.

Fig. 2 shows a schematic model of the human body in a rigid chair. It indicates all the different dimensions and coordinates necessary for the model. Fig. 3 shows the external forces applied to the body. Our model considers gravitation and friction forces.

On applying Newton's law of motion to each segment, the equations of motion can be obtained as follows:

$$
\begin{aligned}
&m_1\ddot{X}_1 = F_{aX} - F_{kX}\\
&m_1\ddot{Y}_1 = F_{aY} - F_{kY} - m_1 g\\
&I_1^G\ddot{\theta}_1 = \{F_{aX}\ell_1 + F_{kX}(L_1-\ell_1)\}\sin\theta_1 - \{F_{aY}\ell_1 + F_{kY}(L_1-\ell_1)\}\cos\theta_1 - \tau_k\\
&m_2\ddot{X}_2 = -F_{BT}\cos\theta_2 - F_{BN}\sin\theta_2 + F_{kX} - F_{hX}\\
&m_2\ddot{Y}_2 = -F_{BT}\sin\theta_2 + F_{BN}\cos\theta_2 + F_{kY} - F_{hY} - m_2 g\\
&I_2^G\ddot{\theta}_2 = -sign(X_2)F_{BN}\sqrt{X_2^{\,2}+Y_2^{\,2}} + F_{kX}\ell_2\sin\theta_2 - F_{kY}\ell_2\cos\theta_2\\
&\qquad + \tau_k - \tau_h + F_{hX}(L_2-\ell_2)\sin\theta_2 - F_{hY}(L_2-\ell_2)\cos\theta_2\\
&m_3\ddot{X}_3 = -F_{CT}\cos\theta_3 - F_{CN}\sin\theta_3 + F_{hX}\\
&m_3\ddot{Y}_3 = -F_{CT}\sin\theta_3 + F_{CN}\cos\theta_3 + F_{hY} - m_3 g\\
&I_3^G\ddot{\theta}_3 = sign(L_\gamma\sin\theta_r - Y_3)F_{CN}\sqrt{(L_\beta + L_\gamma\cos\theta_r - X_3)^2 + (L_\gamma\sin\theta_r - Y_3)^2}\\
&\qquad + F_{hX}\ell_3\sin\theta_3 - F_{hY}\ell_3\cos\theta_3 + \tau_h
\end{aligned}
\tag{1}
$$

where m_i and $I_i^G, i = 1,2,3$ are the mass and mass moment of inertia for the i-th segment, respectively. $(X_i, Y_i), i = 1,2,3$ are the coordinates of the i-th segment. The lower case subscripts a, k, and h on the forces, F, and torques, τ, denote the ankle, knee, and hip joints, respectively. The capital subscripts B and C denote the corresponding contact points, as indicated in Fig. 3. The subscripts T and N represent tangential and normal forces, respectively. All the other parameters that appear in equation (1) are shown in Fig. 2. The tangential forces at the edges of the seat bottom and back are friction forces that are proportional to the corresponding normal forces:

$$F_{BT} = \mu_B F_{BN}, \quad F_{CT} = \mu_C F_{CN}, \tag{2}$$

where μ_B and μ_C are the friction coefficients at the corresponding contact point, *i.e.*, between the user and the seat bottom, and between the user and the seat back, respectively.

The nine equations in equation (1) comprise ten unknown forces and moments, implying that the system is mathematically indeterminate. One way to avoid indeterminacy is to measure one of the unknown variables. In this paper, one unknown force component is measured using the procedure described in detail in the next section.

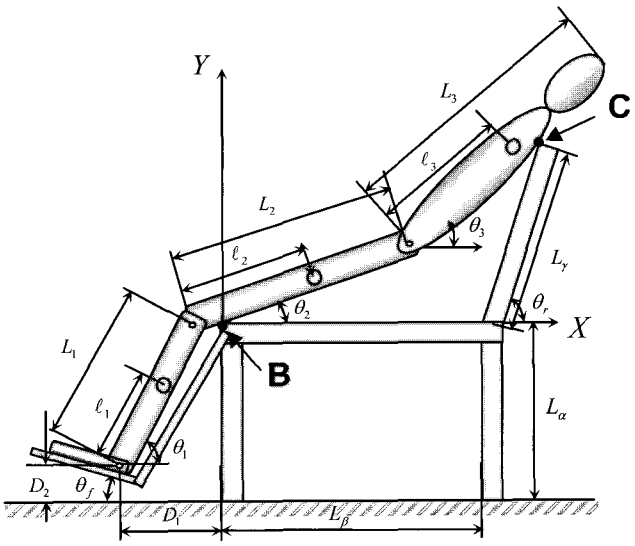

Fig. 2 Schematic model of the human body on a rigid chair

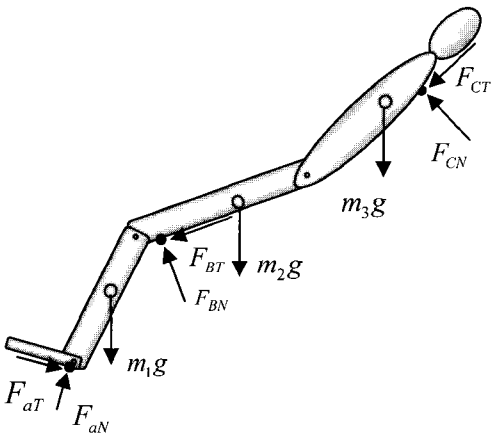

Fig. 3 External forces acting on the human body

Based on the geometric relations, the following kinematic relations can be derived:

$$
\begin{aligned}
&X_1 = \ell_1\cos\theta_1 - D_1,\ Y_1 = \ell_1\sin\theta_1 - (L_\alpha - D_2)\\
&X_2 = L_1\cos\theta_1 + \ell_2\cos\theta_2 - D_1,\ Y_2 = L_1\sin\theta_1 + \ell_2\sin\theta_2 - (L_\alpha - D_2)\\
&X_3 = X_2 + (L_2-\ell_2)\cos\theta_2 + \ell_3\cos\theta_3,\\
&Y_3 = Y_2 + (L_2-\ell_2)\sin\theta_2 + \ell_3\sin\theta_3\\
&\theta_2 = \tan^{-1}\frac{Y_2}{X_2},\ \theta_3 = \tan^{-1}\frac{L_\gamma\sin\theta_r - L_2\sin\theta_2 + (L_\alpha - D_2 - L_1\sin\theta_1)}{L_\beta + L_\gamma\cos\theta_r - L_2\cos\theta_2 + (D_1 - L_1\cos\theta_1)}
\end{aligned}
\tag{3}
$$

As seen in equation (3), there are eight kinematic constraints, but nine coordinates. This leaves only one independent degree of freedom, implying that measuring one coordinate provides all the other coordinates based on the kinematic relationships. With the position information, one can obtain the velocity and acceleration data just by analytical differentiation of the kinematic relations given in equation (3). These expressions are listed in the appendix. The kinematic relations described in equation (3) and the appendix are very useful for estimating the accelerations used for the inverse dynamic analysis.

2.2 Force Identification Method: Inverse Dynamic Approach

Consider the normal and tangential force components at the footrest, F_{aN} and F_{aT}. These components at the footrest can be expressed as

$$F_{aX} = F_{aN}\sin\theta_f + F_{aT}\cos\theta_f, \quad F_{aY} = F_{aN}\cos\theta_f - F_{aT}\sin\theta_f, \tag{4}$$

where θ_f is the footrest angle, as shown in Fig. 3. Nevertheless, in this case, the system is mathematically indeterminate, *i.e.*, the number of unknown forces and moments exceeds the number of equations. Therefore, one unknown variable must be measured or removed to solve the equations directly.

If there is no contact between the user and the seat bottom, then F_{BN} vanishes. In this case, the equations of motion can be rearranged to provide a mathematically determinate equation, which does not require any measurement for the unknown forces to obtain a solution: *i.e.*, equation (1) can be rearranged to give

$$\underset{9\times 9}{[G_1]}\ \underset{9\times 1}{\{F_1\}} = \underset{9\times 1}{\{Q_1\}}, \tag{5}$$

where

$$\{F_1\} = \{F_{aN}\ F_{aT}\ F_{kX}\ F_{kY}\ F_{hX}\ F_{hY}\ F_{CN}\ \tau_k\ \tau_h\}^T,$$

$$\{Q_1\} = \{(m_1\ddot{X}_1)\ (m_1 g + m_1\ddot{Y}_1)\ (I_1^G\ddot{\theta}_1)\ (m_2\ddot{X}_2)\ (m_2 g + m_2\ddot{Y}_2)\ (I_2^G\ddot{\theta}_2)\ (m_3\ddot{X}_3)\ (m_3 g + m_3\ddot{Y}_3)\ (I_3^G\ddot{\theta}_3)\}^T,$$

and the system matrix $[G_1]$ is provided in the appendix. The adequacy of the model in the proposed force identification method will be validated using equation (5) by comparing the estimated and measured normal force F_{aN}.

Of the unknown forces and moments, the normal force at the footrest, F_{aN}, is the easiest force to measure. In this paper, F_{aN} is measured and used to estimate the other forces and moments. If F_{aN} is measurable, equation (1) can be rearranged to give

$$\underset{9\times 9}{[G_2]}\ \underset{9\times 1}{\{F_2\}} = \underset{9\times 1}{\{Q_2\}}, \tag{6}$$

where

$$\{F_2\} = \{F_{aT}\ F_{kX}\ F_{kY}\ F_{BN}\ F_{hX}\ F_{hY}\ F_{CN}\ \tau_k\ \tau_h\}^T,$$

$$\{Q_2\} = \{(-F_{aN}\sin\theta_f + m_1\ddot{X}_1)\ (m_1 g - F_{aN}\cos\theta_f + m_1\ddot{Y}_1)\ \ldots\ (F_{aN}\ell_1\cos(\theta_1+\theta_f) + I_1^G\ddot{\theta}_1)\ (m_2\ddot{X}_2)\ (m_2 g + m_2\ddot{Y}_2)\ldots\ (I_2^G\ddot{\theta}_2)\ (m_3\ddot{X}_3)\ (m_3 g + m_3\ddot{Y}_3)\ (I_3^G\ddot{\theta}_3)\}^T,$$

and $[G_2]$ is given in the appendix. Then, the force vector that includes unmeasured human-generated force components can be obtained easily by solving the linear equation (6).

The parameters used to describe the human body in the model affect the inverse dynamic analysis results. Therefore, accurate parameters are essential to estimate forces accurately. There are some existing empirical formulae based on cadaver studies or computer modeling techniques.[12,13] In this study, we adopted the well-known regression formulae suggested by Zatsiorsky and Seluyanov.[13]

3. Experiments and Results

3.1 Experimental Setup

Fig. 4 shows the experimental setup used to allow measurements of chair forces and human body motion during an extensor thrust event[15]. The experimental system consisted of a wheelchair seat with a footrest, a force plate, a general-purpose digital video camera, a data-acquisition system, and a PC. The chair had adjustable joint angles and the length of the leg rest was also adjustable.

The force plate, equipped with strain gages, was used to measure the normal foot force at the footrest. The digital video camera was used to obtain the human body motion. Fig. 5 shows a sequence of digital image frames taken during an extensor thrust experiment. As the figure shows, markers were attached to the human subject. Human body motion angles were extracted by tracking the markers attached to the human subject using a digital video camera. To synchronize the video measurements with the force measurement, a LED was triggered simultaneously with the onset of force measurement. In the upper left corner of each frame, the LED identifies the starting point of the experiment. There were five markers, and these were attached at two joints of interest, the knee and hip, as well as the elbow, shoulder, and head. The marker motions were tracked digitally to determine the position data for each link of the human subject. Fig. 6 shows the typical marker trajectories during an extensor thrust event.

3.2 Experimental Validation of the Model

The main goal of this preliminary experiment was to establish the validity of the proposed modeling method. An extensor thrust experiment was performed using an intentional motion that breaks contact between the human subject and the seat bottom, so that equation (5) governs this case. Then, no force measurement is needed. The measured angular displacements for this experiment are shown in Fig. 7. In this analysis, all three angular displacements, θ_1, θ_2, and θ_3, were curve-fitted with fourth-order polynomials and used to compute the other coordinates from the kinematic relationships. The linear and angular acceleration data used for force estimation were obtained by analytical differentiation of the fourth-order polynomials of angles and the kinematic relationships.

Fig. 8 compares the measured and estimated normal forces (F_{aN}) at the footrest. These are in a good agreement, except for some minor fluctuation. The fluctuation in the measured force appears to have been caused mainly by an uneven surface and the dynamics of the chair, which rarely affect human body motion. Some modeling error may also have affected this fluctuation. The accuracy of the estimated forces is dependent on the accuracy of the parameters used in the model.

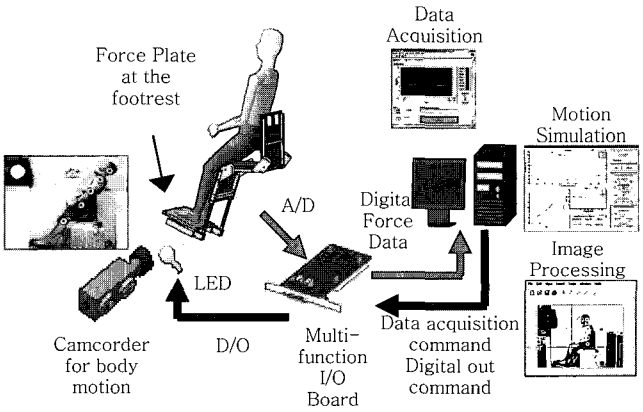

Fig. 4 Schematic diagram of the experimental setup[14]

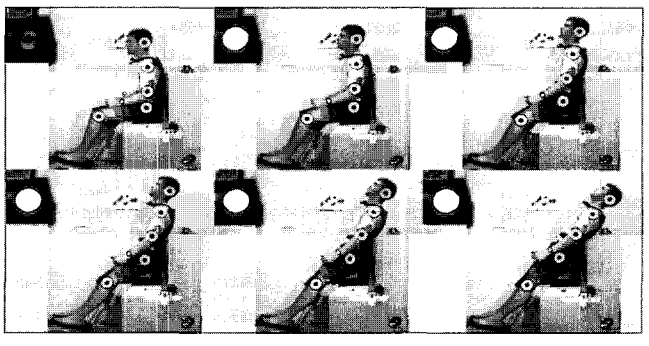

Fig. 5 Progression of an extensor thrust experiment

The friction coefficient is one of the most difficult parameters to identify. Simulations were performed to examine the sensitivity of the results with respect to the friction coefficient between the human subject and the seat back. Fig. 8 also shows the changes in the predicted normal foot force when the friction coefficient, μ_C, was changed by ±0.1 from the nominal value of 0.3. An increase or decrease in the friction coefficient shifted the estimation somewhat, although the estimation still fell in an acceptable region. Therefore, the assumptions introduced to establish the model were acceptable.

3.3 Extensor Thrust Test

The experiments in this section were intended to test the performance of the proposed method for estimating the human-generated forces during extensor thrust events. First, an experiment was conducted to test the adequacy of the proposed method for a typical extensor thrust event. In this experiment, the footrest and seat back angles were set to 15° and 90°, respectively. Fig. 9 compares the sets of measured and estimated angular displacements based on the kinematic relationships, as discussed in the previous chapter. In general, only one angular displacement was required to estimate the other coordinates, and the angular displacement θ_2 was used to estimate the other coordinates.

Fig. 9 shows that the estimated angles were close to the measured angles, although θ_1 and θ_3 were somewhat underestimated and overestimated, respectively. These errors appear to have been due to the shapes of the thigh and back, but did not significantly affect the force identification. Two sets of reaction forces, which were identified by using only measured angles and by using two estimated angles and one measured angle, are presented in Fig. 10.

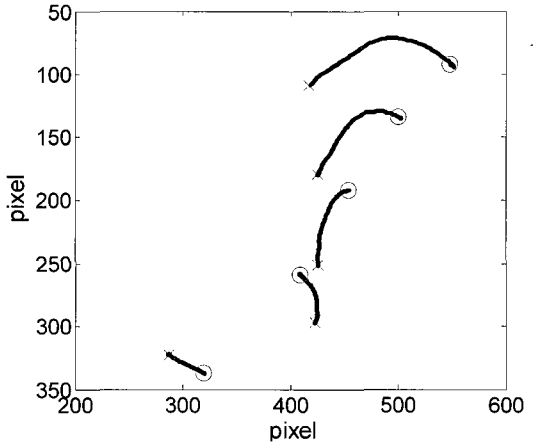

Fig. 6 Typical marker trajectories

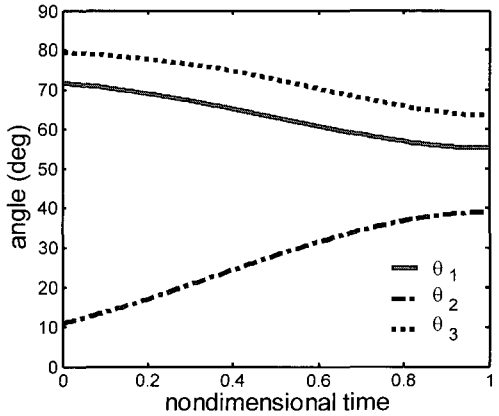

Fig. 7 Measured angular displacements for the model validation experiment

The identified forces included the tangential force (F_{aT}) at the footrest and the normal forces on the seat bottom (F_{BN}) and back (F_{CN}). The comparison of the two sets of identified forces confirmed that the forces estimated with a combination of measured and estimated angles were in good agreement with those using measured angles only. Therefore, the derived kinematic results were sufficient to represent the kinematic behavior of the system.

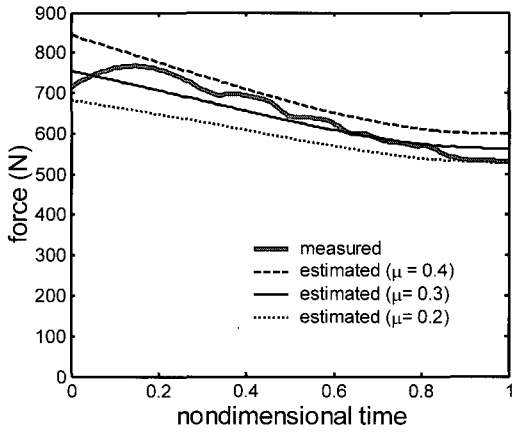

Fig. 8 Comparison of the measured and simulated normal foot forces in the model validation experiment

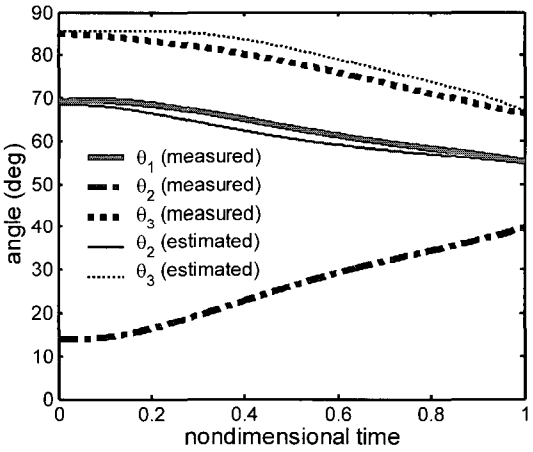

Fig. 9 Measured and estimated angular displacements: footrest angle = 15°, seat back angle = 90°

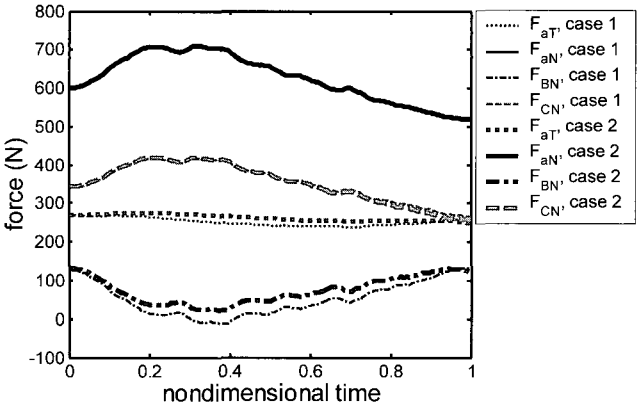

Fig. 10 The forces identified using two different sets of angular displacement: case 1, using only measured angular displacements; case 2, using one measured and two estimated angular displacements; footrest angle = 15°, seat back angle = 90°

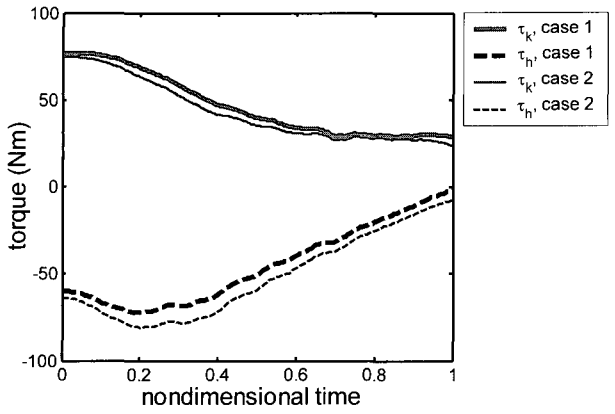

Fig. 11 Torques identified using two different sets of angular displacements: case 1, using only measured angular displacements; case 2, using one measured and two estimated angular displacements; foot rest angle = 15°, seatback angle = 90°

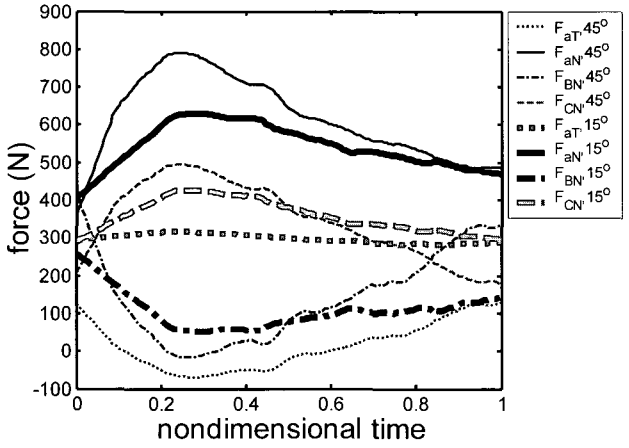

Fig. 12 Forces identified while changing the footrest angle from 15° to 45°; seat back angle = 80°

The identified torques at the knee (τ_k) and hip (τ_h) joints are shown in Fig. 11, which also shows that there was no significant difference in identification between using measured angles only and using a combination of estimated and measured angles

To show the effects of the chair configuration, two experiments were conducted that involved changing the footrest and seat back angles. Figs 12 and 13 show the identified forces and torques from these experiments. Comparison of Figs. 10 and 12 revealed that a change in seat back angle from 90° to 80° decreased the normal force at the footrest slightly, but increased the tangential force at the footrest, because more tangential force at the footrest was required to compensate for the increase in horizontal reaction force from the seat back. Fig. 12 shows that the increase in the footrest angle makes it easy to produce a horizontal force by increasing the normal foot force. In this case, the tangential foot force decreased drastically, while the normal force increased. Fig. 13 shows that the joint torques were also affected by the change in the footrest angle.

Overall, the normal force at the footrest was relatively significant and was the dominant force driving the extension motion, while the tangential force was less important, but increased as the extension progressed.

Fig. 14 shows the human-generated forces when an artificial disturbance was engaged, *i.e.*, the human subject intentionally rocked during the extensor thrust event. The force and torque patterns were quite different from those in the other experiments due to the major change in the angular displacement patterns. However, the peak values were not greatly different from the others, implying that the inertial effects were not dominant in this case.

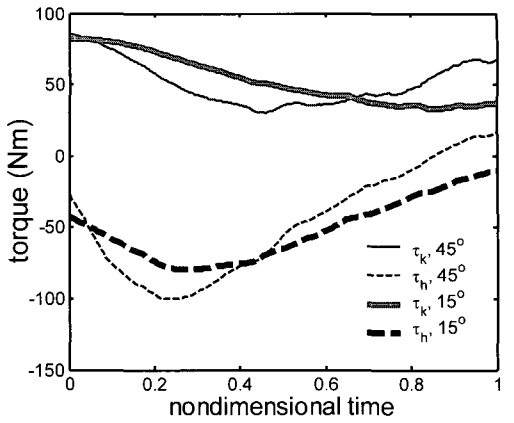

Fig. 13 Torques identified for different footrest angles from 15° to 45°; seat back angle = 80°

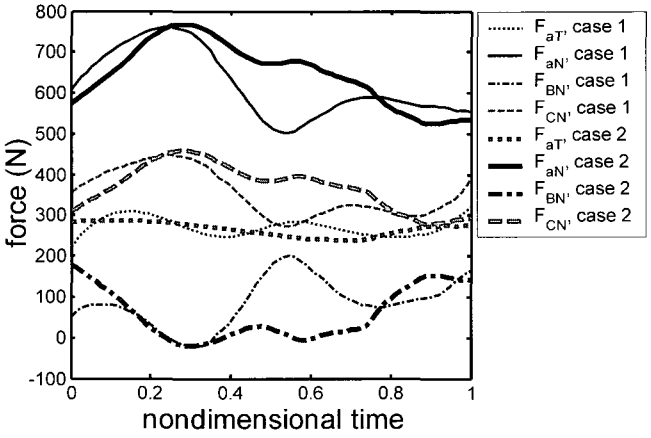

Fig. 14 Comparison of the identified forces with and without intentional rocking motion during an extensor thrust event; footrest angle = 15°, seat back angle = 80°. Case 1, with rocking motion; case 2, without rocking motion

4. Conclusions

We propose a novel method to identify the human-generated forces during extensor thrust events. We developed an experimental system to measure the angular motion of the human body and the forces at the footrest, using an inverse dynamic approach along with a three-link human body model. Measurements at the footrest were used to overcome the mathematical indeterminacy of the problem. The proposed method was verified in several extensor thrust experiments, and this new method should be useful for developing performance specifications and evaluation methods of wheelchair design for people with pronounced extensor thrust.

REFERENCES

1 Cooper, R. A., "Advances in wheelchair and related technologies," Medical Engineering & Physics, Vol. 23, pp. 3-4, 2001.

2 Zeltwanger, A. P., Brown, D. and Bertocci, G., "Utilizing computer modeling in the development of a dynamic seating system," Proceedings of the 24th RESNA, Reno, NV, USA, 2001.

3 InterCo GmbH Web site, http://www.interco-reha.de

4 Miller's Adaptive Technologies, Product Catalog, 2004.

5 Pandyan, A. D., Price, C. I. I. M., Rodgers, H., Barnes, M. P. and Johnson, G. R., "Biomechanical examination of a commonly used measure of spasticity," Clinical Biomechanics, Vol. 16, pp. 859-

865, 2001.

6 Lebiedowska, M. K. and Fisk, J. R., "Passive dynamics of the knee joint in healthy children and children affected by spastic paresis," Clinical Biomechanics, Vol. 14, pp. 653-660, 1999.

7 Simon, D. and Foulds, R., "Developing a quantitative measure of muscle spasticity," Proceedings of the IEEE 30th Annual Northeast Bioengineering Conference, Springfield, MA, USA, 2004.

8 Hutchinson, E. B., Riley, P. O. and Krebs, D. E., "A dynamic analysis of the joint forces and torques during rising from a chair," IEEE Trans. Rehabilitation Engineering, Vol. 2, No. 2, pp. 49-56, 1994.

9 Sibella, F., Galli, M., Romei, M., Montesano, A. and Crivellini, M., "Biomechanical analysis of sit-to-stand movement in normal and obese subjects," Clinical Biomechanics, Vol. 18, pp. 745-750, 2003.

10 Mak, M. K. Y., Levin, O., Mizrahi, J. and Hui-Chan, C. W. Y., "Reduction of lower limb model indeterminacy by force redundancy in sit-to-stand motion," Journal of Applied Biomechanics, Vol. 20, pp. 95-102, 2004.

11 Yamaguchi, G. T., Moran, D. W. and Si, J., "A computationally efficient method for solving the redundant problem in biomechanics," Journal of Biomechanics, Vol. 28, No. 8, pp. 999-1005, 1995.

12 Nigg, B. M. and Herzog, W., "Biomechanics of the musculo-skeletal System," John Wiley & Sons, New York, NY, USA, 1995.

13 Zatsiorsky, V. and Seluyanov, V., "Estimation of the mass and inertia characteristics of the human body by means of the best predictive regression equations," International Series on Biomechanics, Vol. 5B, pp. 233-239, 1985.

14 Hong, S. W., Patrangenaru, V., Singhose, W. and Sprigle, S., "Motion measurement and force determination during unconstrained extensor thrust," Proceedings of RESNA 2005, Atlanta, GA, USA, 2005.

Appendix 1: The kinematic relationships for velocity and acceleration

$$\dot{X}_1 = -\ell_1 \sin\theta_1\dot{\theta}_1$$
$$\dot{Y}_1 = \ell_1 \cos\theta_1\dot{\theta}_1$$
$$\dot{X}_2 = -L_1 \sin\theta_1\dot{\theta}_1 - \ell_2 \sin\theta_2\dot{\theta}_2$$
$$\dot{Y}_2 = L_1 \cos\theta_1\dot{\theta}_1 + \ell_2 \cos\theta_2\dot{\theta}_2$$
$$\dot{X}_3 = \dot{X}_2 - (L_2 - \ell_2)\sin\theta_2\dot{\theta}_2 - \ell_3 \sin\theta_3\dot{\theta}_3$$
$$\dot{Y}_3 = \dot{Y}_2 + (L_2 - \ell_2)\cos\theta_2\dot{\theta}_2 + \ell_3 \cos\theta_3\dot{\theta}_3$$
$$\ddot{X}_1 = -\ell_1 \cos\theta_1(\dot{\theta}_1)^2 - \ell_1 \sin\theta_1\ddot{\theta}_1$$
$$\ddot{Y}_1 = -\ell_1 \sin\theta_1(\dot{\theta}_1)^2 + \ell_1 \cos\theta_1\ddot{\theta}_1$$
$$\ddot{X}_2 = -L_1 \cos\theta_1(\dot{\theta}_1)^2 - L_1 \sin\theta_1\ddot{\theta}_1 - \ell_2 \cos\theta_2(\dot{\theta}_2)^2 - \ell_2 \sin\theta_2\ddot{\theta}_2$$
$$\ddot{Y}_2 = -L_1 \sin\theta_1(\dot{\theta}_1)^2 + L_1 \cos\theta_1\ddot{\theta}_1 - \ell_2 \sin\theta_2(\dot{\theta}_2)^2 + \ell_2 \cos\theta_2\ddot{\theta}_2$$
$$\ddot{X}_3 = \ddot{X}_2 - (L_2 - \ell_2)\cos\theta_2(\dot{\theta}_2)^2 - (L_2 - \ell_2)\sin\theta_2\ddot{\theta}_2 - \ell_3 \cos\theta_3(\dot{\theta}_3)^2 - \ell_3 \sin\theta_3\ddot{\theta}_3$$
$$\ddot{Y}_3 = \ddot{Y}_2 - (L_2 - \ell_2)\sin\theta_2(\dot{\theta}_2)^2 + (L_2 - \ell_2)\cos\theta_2\ddot{\theta}_2 - \ell_3 \sin\theta_3(\dot{\theta}_3)^2 + \ell_3 \cos\theta_3\ddot{\theta}_3$$

$$\dot{\theta}_2 = \cos^2\theta_2 \frac{X_2\dot{Y}_2 - \dot{X}_2 Y_2}{X_2^2},\ \dot{\theta}_3 = \cos^2\theta_3 \frac{X_C\dot{Y}_C - \dot{X}_C Y_C}{X_C^2},$$

$$\ddot{\theta}_2 = \frac{\cos^2\theta_2(X_2\ddot{Y}_2 - \ddot{X}_2 Y_2) - \sin 2\theta_2\dot{\theta}_2(X_2\dot{Y}_2 - \dot{X}_2 Y_2) - 2X_2\dot{X}_2\dot{\theta}_2}{X_2^2},$$

$$\ddot{\theta}_3 = \frac{\cos^2\theta_3(X_C\ddot{Y}_C - \ddot{X}_C Y_C) - \sin 2\theta_3\dot{\theta}_3(X_C\dot{Y}_C - \dot{X}_C Y_C) - 2X_C\dot{X}_C\dot{\theta}_3}{X_C^2}$$

where

$$X_C = L_\beta + L_\gamma \cos\theta_r - (L_1 \cos\theta_1 + L_2 \cos\theta_2 - D_1)$$
$$Y_C = L_\gamma \sin\theta_r - (L_1 \sin\theta_1 + L_2 \sin\theta_2 - (L_\alpha - D_2))$$

Appendix 2: System matrices

$[G_1]$:

$G_{11} = \sin\theta_f, G_{12} = \cos\theta_f, G_{13} = -1, G_{21} = \cos\theta_f, G_{22} = -\sin\theta_f, G_{24} = -1,$
$G_{31} = -\ell_1 \cos(\theta_1 + \theta_f), G_{32} = \ell_1 \sin(\theta_1 + \theta_f), G_{33} = (L_1 - \ell_1)\sin\theta_1, G_{34} = -(L_1 - \ell_1)\cos\theta$
$G_{38} = -1, G_{43} = 1, G_{45} = -1, G_{54} = 1, G_{56} = -1, G_{63} = \ell_2 \sin\theta_2, G_{64} = -\ell_2 \cos\theta_2,$
$G_{65} = (L_2 - \ell_2)\sin\theta_2, G_{66} = -(L_2 - \ell_2)\cos\theta_2, G_{68} = 1, G_{69} = -1, G_{75} = 1,$
$G_{77} = -D_{CX}, G_{86} = 1, G_{87} = -D_{CY}, G_{95} = \ell_3 \sin\theta_3,$
$G_{96} = -\ell_3 \cos\theta_3, G_{97} = L_\delta, G_{99} = 1,$ *the other elements* $= 0.$

$[G_2]$:

$G_{11} = \cos\theta_f, G_{12} = -1, G_{21} = -\sin\theta_f, G_{23} = -1, G_{31} = \ell_1 \sin(\theta_1 + \theta_f),$
$G_{32} = (L_1 - \ell_1)\sin\theta_1, G_{33} = -(L_1 - \ell_1)\cos\theta_1, G_{38} = -1, G_{42} = 1,$
$G_{44} = -D_{BX}, G_{45} = -1, G_{53} = 1, G_{54} = -D_{BY},$
$G_{56} = -1, G_{62} = \ell_2 \sin\theta_2, G_{63} = -\ell_2 \cos\theta_2, G_{64} = -sign(X_2)\sqrt{X_2^2 + Y_2^2},$
$G_{65} = (L_2 - \ell_2)\sin\theta_2, G_{66} = -(L_2 - \ell_2)\cos\theta_2, G_{68} = 1, G_{69} = -1, G_{75} = 1,$
$G_{77} = -D_{CX}, G_{86} = 1, G_{87} = -D_{CY}, G_{95} = \ell_3 \sin\theta_3,$
$G_{96} = -\ell_3 \cos\theta_3, G_{97} = L_\delta, G_{99} = 1,$ *the other elements* $= 0.$

where

$$D_{BX} = \mu_B \cos\theta_2 + \sin\theta_2,\ D_{BY} = \mu_B \sin\theta_2 - \cos\theta_2,$$
$$D_{CX} = \mu_C \cos\theta_3 + \sin\theta_3,\ D_{CY} = \mu_C \sin\theta_3 - \cos\theta_3,$$
$$L_\delta = sign(L_\gamma \sin\theta_r - Y_3)\sqrt{(L_\beta + L_\gamma \cos\theta_r - X_3)^2 + (L_\gamma \sin\theta_r - Y_3)^2}$$